Drug Design, Development and Therapy

Dovepress
Taylor & Francis Group

Open Access Full Text Article

ORIGINAL RESEARCH

Population Pharmacokinetic Analyses and Exposure–Efficacy Relationships of Venetoclax in Chinese Pediatric Patients with Hematological Malignancy in a Real-World Setting

Yinyu Zhao[1,2,*], Xuchen Song[1,3,*], Lin Zhang[4], Yidan Zhu[1,2], Jiali Chen[1,3], Yiru Gong[1,2], Xingxian Luo[1], Huan He[5], Xiaohong Zhang[1], Lin Huang[1]

[1]Department of Pharmacy, Peking University People's Hospital, Beijing, People's Republic of China; [2]School of Pharmaceutical Sciences, Peking University, Beijing, People's Republic of China; [3]School of Clinical Pharmacy, Shenyang Pharmaceutical University, Shenyang, People's Republic of China; [4]Department of Pediatrics, Peking University People's Hospital, Beijing, People's Republic of China; [5]Department of Pharmacy, Beijing Children's Hospital of Capital Medical University, Beijing, People's Republic of China

*These authors contributed equally to this work

Correspondence: Lin Huang, Department of Pharmacy, Peking University People's Hospital, No. 11 Xizhimen South Street, Xicheng District, Beijing, 100044, People's Republic of China, Email huanglin@pkuph.edu.cn

Background: Venetoclax (VEN), a selective B-cell lymphoma 2 (BCL-2) inhibitor, is used in pediatric hematologic malignancies. Research on individualized VEN therapy in Chinese pediatric patients remains limited. This study aimed to develop a population pharmacokinetic (PPK) model in Chinese pediatric patients, identify covariates influencing pharmacokinetics, support personalized dosing, and explore exposure-efficacy relationships in pediatric acute myeloid leukemia (AML).

Methods: PPK modeling was based on 225 plasma concentrations from 96 patients using nonlinear mixed-effects (NLME) modeling in Phoenix NLME software. A retrospective cohort of 52 AML patients receiving VEN with hypomethylating agents was analyzed, grouped as newly diagnosed or relapsed/refractory (R/R). Minimal residual disease (MRD) negativity was the primary endpoint. Mann–Whitney *U*-tests and logistic regression assessed associations between trough concentration (C_0) and 6-hour post-dose concentration (C_6) levels and MRD status.

Results: A one-compartment model best described the pharmacokinetics of VEN. Body surface area (BSA) and the use of triazole drugs significantly influenced apparent clearance (CL/F), while total protein (TP) had a significant impact on apparent volume of distribution (V/F). The final model estimates were: ka = 0.15 h^{-1} (fixed), V/F = 124.7 L, CL/F = 4.8 $L \cdot h^{-1}$. In both newly diagnosed and R/R AML patients, C_0 and C_6 concentrations were significantly higher in the MRD-negative group than in the MRD-positive group (all $p < 0.05$). Exposure–response analyses demonstrated a consistent positive association between higher VEN exposure and MRD negativity. Logistic regression further confirmed that both C_0 and C_6 were independent predictors of achieving MRD negativity. Notably, in the R/R cohort, higher C_6 exposure quartiles were significantly associated with increased MRD-negative rates.

Conclusion: This study establishes the first real-world population pharmacokinetic model of venetoclax in Chinese pediatric patients and demonstrates a clinically meaningful exposure–response relationship. The positive association between VEN exposure and MRD negativity supports the use of therapeutic drug monitoring and PPK-guided dosing to optimize treatment in pediatric AML.

Keywords: venetoclax, pediatric, hematological malignancy, population pharmacokinetics

Background

Venetoclax (VEN), a selective and potent B-cell lymphoma 2 (BCL-2) inhibitor, is approved for the treatment of adults with chronic lymphocytic leukemia (CLL) or small lymphocytic lymphoma (SLL) and acute myeloid leukemia (AML).[1] However, numerous Phase 1 trials have been conducted to assess the combination of venetoclax with standard treatments

https://doi.org/10.2147/DDDT.S583847
Received: 19 December 2025
Accepted: 1 March 2026
Published: 20 March 2026

in pediatric, adolescent, and young adult populations suffering from relapsed or refractory (R/R) malignancies.[2–4] These studies demonstrated encouraging clinical activity, with overall response rates of 60–80% and manageable toxicity profiles, supporting the expanding off-label and guideline-recommended use of VEN in children with R/R hematologic malignancies. In addition, retrospective studies and real-world pediatric cohorts have further supported its clinical feasibility,[5–7] and VEN has been incorporated into relevant treatment guidelines.[8,9]

Clinical application reveals substantial inter- and intra-individual variability in VEN exposure.[10–12] Adult studies demonstrate a correlation between drug exposure levels and clinical outcomes[13–15] (eg, minimal residual disease (MRD) negativity), underscoring the imperative for individualized dosing regimens based on patient-specific factors. However, fundamental pharmacokinetic (PK) differences between children and adults—including distinct drug-metabolizing enzyme activity, body composition distribution, and clearance rates—combined with divergent disease profiles and comedication patterns preclude direct extrapolation of adult dosing strategies to pediatric populations. Moreover, ethnic variability in CYP3A5 polymorphisms, which may influence venetoclax metabolism, could further contribute to inter-population differences in drug exposure. Therefore, pharmacokinetic studies of VEN in children are warranted.

VEN's intrinsic PK properties further contribute to exposure variability: as a substrate of CYP3A4, P-glycoprotein, and breast cancer resistance protein (BCRP), its absorption and metabolism are susceptible to hepatic/renal function, concomitant medications, and dietary conditions;[16] high plasma protein binding (>99%, unbound fraction <0.01) restricts tissue distribution;[17] and predominant hepatic metabolism results in unique kinetic behaviors within children's developing metabolic systems.[16] Although adult studies have linked VEN steady-state trough concentrations (C_0) to MRD negativity, with higher MRD-negative rates observed at normal C_0 levels (90.91% vs 33.33%, p=0.028),[18] pediatric studies by Badawi et al reported a flat exposure–efficacy relationship.[19] This discrepancy may reflect developmental-stage-specific exposure-response dynamics. Therefore, in addition to trough concentrations (C0), peak concentrations (C6, sampled 6 ± 0.5 hours post-dose) were selected as parameters of interest. Venetoclax typically reaches peak plasma levels 5–8 hours after oral administration, making C6 a practical surrogate for Cmax. Evaluating both C0 and C6 enables assessment of steady-state and peak exposure, which may better capture variability in absorption, the influence of concomitant CYP3A inhibitors (eg, azole antifungals), and potential associations with treatment response in pediatric patients.

Critical evidence gaps persist in pediatric precision dosing of VEN. To date, the limited population pharmacokinetic (PPK) models of venetoclax are primarily based on adult populations, particularly the elderly,[20] with only one study including pediatric-to-adolescent patients.[19] Significant research gaps remain regarding pediatric populations, especially in Chinese cohorts. Moreover, most published studies derive from well-controlled clinical trials, resulting in limited real-world evidence. There is a need to design a tailored VEN dosage regimen for Chinese pediatric patients. In addition, a previous study from our research program evaluated the clinical efficacy and safety of venetoclax-based regimens in pediatric patients with R/R acute lymphoblastic leukemia, without pharmacokinetic analyses or exposure–response evaluation.[21] In contrast, the present study focuses on population pharmacokinetics, exposure–efficacy relationships, and individualized dosing optimization of venetoclax in a larger and more heterogeneous cohort of Chinese pediatric patients with hematological malignancies, primarily acute myeloid leukemia, using real-world therapeutic drug monitoring data. Therefore, this real-world PPK study aims to characterize the pharmacokinetic profile of VEN in Chinese pediatric patients, elucidate sources of interindividual variability, investigate exposure–response associations, and ultimately provide a foundation for individualized dosing strategies, as well as support exposure prediction and monitoring during dose optimization.

Methods

Patients

This study was conducted in accordance with the Declaration of Helsinki and approved by the Ethics Committee of Peking University People's Hospital (Approval No. 2022PHB095-001). Written informed consent was obtained from the parents or legal guardians of all pediatric participants prior to enrollment. All patient data were anonymized and handled confidentially.

Patients in Population Pharmacokinetic Model

The study comprised pediatric patients who underwent venetoclax therapeutic drug monitoring (TDM) at Peking University People's Hospital between December 2021 and December 2024. The inclusion criteria were restricted to pediatric patients, while the exclusion criteria encompassed adult patients and those lacking relevant clinical data in their electronic medical records. Patient demographic details and laboratory results were extracted from electronic health records and routine follow-up documentation. These variables included age, sex, height, weight, body surface area (BSA), ethnicity, venetoclax dosage, concurrent use of triazoles, venetoclax administration frequency, treatment duration, timing of venetoclax intake, timing of blood sampling, as well as hematological parameters such as complete blood count with differential, lymphocyte percentage (LY%), hemoglobin (HGB), platelet count (PLT), total protein (TP), total bilirubin (TBIL), creatinine (CRE), estimated glomerular filtration rate (eGFR), total carbon dioxide (TCO2), and lactate dehydrogenase (LDH). The estimated glomerular filtration rate (eGFR) was derived using the CKD-EPI formula to assess renal function.[22]

Patients in Exposure-Efficacy Analysis

The study encompassed pediatric patients with a confirmed diagnosis of acute myeloid leukemia (AML) who received venetoclax (VEN) in combination with hypomethylating agents (HMAs), including azacitidine or decitabine, and who underwent therapeutic drug monitoring (TDM) at Peking University People's Hospital between December 2022 and April 2025. For the purpose of the exposure-efficacy analysis, patients were stratified into two distinct groups based on their disease status: those with newly diagnosed AML and those with R/R AML. The patients should be eligible for response evaluation. The primary endpoints were minimal residual disease (MRD), with MRD negativity defined as <0.1%.

Study Design

Venetoclax dosing was initiated using a stepwise escalation over a period of 2 to 3 days, culminating in a target maintenance dose ranging from 100 to 400 mg administered once daily. During the course of treatment, the venetoclax dosage was modified based on the patients' therapeutic responses, adverse drug reactions, and/or tolerance levels. Blood samples from outpatient visits were obtained following at least 5 days of continuous administration at the prescribed dose. A sparse sampling approach was utilized for blood collection. Pre-dose blood samples were collected 30 minutes prior to administration to measure the venetoclax trough concentration (22–24 hours post-dose, designated as C_0). The peak concentration was assessed 6 hours after administration (6 ± 0.5 hours, designated as C6). Additionally, blood samples were also collected at 2 hours, 4 hours, 8 hours, and 10 hours following drug administration.

Bioanalytical Methods

The blood samples were mixed with ethylenediamine tetraacetic acid and subsequently centrifuged at 3000 rpm for 10 minutes. Venetoclax plasma concentrations were determined using ultra-high-performance liquid chromatography with a Thermo Hypersil GOLD™ C_{18} column, employing carbamazepine as the internal standard. The lower limit of quantification was 0.1 μg/mL, and the calibration range of 0.1–10 μg/mL exhibited excellent linearity with an r^2 value of 0.9999. This method demonstrated good accuracy and acceptable precision.

Population Pharmacokinetic Modeling

The PPK model was established utilizing a nonlinear mixed-effects modeling framework to describe the pharmacokinetic variability within the study population. This model was constructed employing the first-order conditional estimation with extended least squares (FOCE-ELS) method, implemented via Phoenix NLME software (Version 8.3; Certara, St. Louis, MO). Statistical analyses and graphical representations were also produced using Phoenix NLME software.

Structural Model

The VEN PK data were fitted using a two-compartment model with first-order absorption, consistent with prior PPK studies.[19,20,23] Fixed-effect parameters included apparent volume of distribution (V/F), apparent clearance (CL/F), and absorption rate constant (ka). Due to insufficient absorption data, ka was fixed at 0.15 h^{-1}, as informed by previously

published literature.[23,24] A lognormal distribution was used to explain interindividual variability (η) and covariance, whereas a proportional model described residual error. Model comparison relied on the objective function minimum (≈ −2*Log(Likelihood) (−2LL)) and visual inspection of goodness-of-fit plots.

Covariate Model

The model employed a power function (Eq. 1) to assess the impact of each continuous covariate (age, BSA, LY%, HGB, PLT, TP, TBIL, CRE, eGFR, TCO2, LDH), which were mean-centered. Categorical covariates (population, triazole) were implemented using Equation 2, with reference categories coded as 0 and comparator categories as 1 for dichotomous variables.

$$Pi = P \times (Cov/Mean_{cov})^{\wedge}\theta_{cov} \tag{1}$$

$$Pi = P \times e^{\wedge}(\theta_{cov} \times Cov) \tag{2}$$

Within the model equations, $Mean_{cov}$ denotes the mean of the covariate, while θcov quantifies the magnitude of the covariate's fixed effect on the parameter. During the covariate inclusion phase, potential covariates were evaluated against a statistical threshold of $P < 0.05$, with a requisite reduction in −2LL of at least 3.84 units. Conversely, the removal phase employed a more stringent criterion ($P < 0.001$), requiring a minimum increase in −2LL of 10.3 units upon covariate deletion to justify retention. When encountering multiple collinear variables, one should select a single variable based on clinical relevance and practical applicability. Covariates inducing a shift exceeding ±20% in the estimated pharmacokinetic parameters relative to the base model were deemed clinically significant.

Model Evaluation and Validation

To evaluate the base structural model and final model, we examined goodness-of-fit plots including conditional weighted residuals (CWRES) versus population predictions (PRED), CWRES versus time after dose (TAD), observations (DV) versus PRED, DV versus individual predictions (IPRED), quantile–quantile (QQ) plots of CWRES and histogram of CWRES. In addition, to assess the robustness and predictive accuracy of the final model, both the bootstrap resampling technique and visual predictive check (VPC) were employed. The median parameter estimates derived from the bootstrap procedure, along with their associated 95% confidence intervals (calculated as the 2.5th and 97.5th percentiles from 1000 resamples), were contrasted with the parameter estimates obtained from the finalized model.

Following final model establishment, data obtained from April to December 2024 at Peking University People's Hospital (Beijing, China) were utilized for external evaluation. Individual predicted concentrations (CIPRED) for C6 were derived via Bayesian forecasting, using fixed values for structural and variability parameters as well as C0 from the final estimates, with zero iterations specified. GOF plots were examined visually. The assessment of model bias and precision was conducted through the calculation of the mean prediction error (MPE) and mean absolute error (MAE), which were determined by the following formulas:

$$MPE(\%) = \frac{1}{N}\sum_{i=1}^{N}\left(\frac{C_{OBS} - C_{IPRED}}{C_{OBS}}\right) \tag{3}$$

$$MAE(\%) = \frac{1}{N}\sum_{i=1}^{N}\left|\frac{C_{OBS} - C_{IPRED}}{C_{OBS}}\right| \tag{4}$$

Model adequacy was determined based on predictive performance criteria, requiring MPE below 20% and MAE of no more than 30%, with C_{OBS} denoting observed concentrations and N the number of data points.[25,26]

Exposure-Efficacy Analysis

Pediatric AML patients receiving VEN in combination with a hypomethylating agent (azacitidine or decitabine) were included in the exposure–efficacy analysis. Associations between venetoclax exposures (C_0 and C_6) and MRD negativity

were assessed via quartile-based graphical analysis and further evaluated using the Mann–Whitney *U*-test and logistic regression. Statistical analyses were conducted using SPSS version 29.0.

Results

Patient Characteristics

In this study, the PPK model was developed using 225 plasma concentration data points from 96 patients, with 16 observations excluded due to being below the lower limit of quantification or lacking dosing information. The demographic and clinical characteristics of the enrolled patient are presented in Table 1. The median age of patients was 12 years (range: 0.3–18 years). 33.3% of patients used triazole drugs (Posaconazole or Voriconazole) in combination.

Data from 52 patients were included in the exposure-efficacy analysis, divided into Newly Diagnosed and R/R. The MRD negativity rates were 78.1% and 65.0%, respectively. Refer to Table 2 for detailed information.

Table 1 Demographic Data Summary of Patients Included in Population Pharmacokinetic Analysis

	Number (%)	Mean (SD)	Median (Range)
No. of patients (samples)	96 (225)		
Sex			
Male	47 (49.0)		
Female	49 (51.0)		
Age (year)		11 (4.6)	12 (0.3–18)
Height (cm)		145 (29.8)	156 (63–190)
Weight (kg)		42 (21.2)	45 (8–112)
BMI ($kg \cdot m^{-2}$)		18.4 (4.5)	17.2 (12.4–36.2)
BSA (m^2)		1.27 (0.4)	1.38 (0.33–2.35)
Population			
AML	64 (66.7)		
ALL	20 (20.8)		
MAL	4 (4.2)		
CML	2 (2.1)		
NHL	5 (5.2)		
MDS	1 (1.0)		
White blood cell (10^9/L)		4.67 (11.7)	2.36 (0.01–138.26)
Neutrophil (10^9/L)		1.28 (5.07)	1.1 (0.00–94.8)
Red blood cell (10^{12}/L)		3.10 (0.92)	2.96 (1.08–5.41)
Hemoglobin (g/L)		93.95 (25.96)	91 (33.00–163.00)
Lymphocyte (%)		37.26 (27.80)	37.45 (0.10–100.00)
Platelets (10^9/L)		105.28 (99.91)	71 (3.00–660.00)
Alanine transaminase (U/L)		33.37 (68.38)	19 (4.00–903.00)
Aspartate aminotransferase (U/L)		28.89 (74.98)	19 (4.00–1113.00)
Lactate dehydrogenase (U/L)		416.14 (1036.12)	222 (15.0–14,968.00)
Total protein (g/L)		62.53 (7.50)	62 (39.20–99.40)
Total bilirubin (μmol/L)		14.48 (9.72)	12.4 (2.70–86.10)
Creatinine (μmol/L)		43.79 (25.64)	42 (4.80–299.0)
eGFR ($mL/min \cdot 1.73m^2$)		165.61 (27.98)	162.94 (40.00–266.91)
T-CO_2 (mmol/L)		23.76 (3.18)	23.75 (4–36)
Triazole co-medication			
With	32 (33.3)		
Not with	64 (66.7)		

Abbreviations: BMI, body mass index; BSA, body surface area; AML, Acute myeloid leukemia; ALL, Acute lymphoblastic leukemia; MAL, Mixed lineage acute leukemia; CML, chronic myeloid leukemia; NHL, Non-Hodgkin lymphoma; MDS, Myelodysplastic syndromes; SD, standard deviation.

https://doi.org/10.2147/DDDT.S583847

Population Pharmacokinetic Modeling

The final model adopted a one-compartment structure, incorporating interindividual variability for CL/F and V/F, along with a multiplicative model for residual error. The base model yielded an objective function value (OFV) of 636.3, with estimated parameters for CL/F and V/F at 2.1 L/h and 105.7 L, respectively (Supplementary Table S1).

Through forward selection and backward elimination of all variables, it was determined that BSA and Triazole significantly influenced CL/F, while TP significantly affected V/F. These factors were incorporated into the final PPK model. The addition of these covariates led to a substantial reduction in the OFV, from 636.3 to 586.8 (ΔOFV = −49.5). Furthermore, the inclusion of covariates accounted for part of the random interindividual variability (IIV) in the population parameters, with the IIV for CL/F decreasing from 1.168 in the base model to 0.996 in the final model. The final model, incorporating the three covariates, is described as follows:

$$V/F = 124.7 \times (TP/62)^{1.7} \tag{5}$$

$$CL/F = 4.8 \times (BSA/1.27)^{1.4} \times e^{(-1.1 \times Triazole)} \tag{6}$$

The typical values for V/F and CL/F are 124.7 L and 4.8 $L \cdot h^{-1}$, respectively. The mean values for TP and BSA are 62 $g \cdot L^{-1}$ and 1.27 m^2, respectively. The coefficients for TP and BSA are 1.7 and 1.4, respectively. If triazole is used, the Triazole value is equal to 1, otherwise it is equal to 0. The final PK model, detailed in Table 3, demonstrates acceptable parameter estimation precision, with relative standard errors (RSE%) ranging from −34.4% to 26.5%.

Model Evaluation and Validation

Figure 1 displays the goodness-of-fit assessments for the final model, showing no significant systematic deviations, which indicates that the model accurately captures the pharmacokinetics of VEN in the study population. Table 3 presents the median parameter estimates obtained through the bootstrap procedure, along with their corresponding 95% CIs. The typical values from the final model closely resembled those obtained from 1000 successful bootstrap replications, and the 95% CIs included the parameter estimates from the final model, indicating robust model stability. Additionally, the VPC in Figure 2 demonstrated that the majority of the observed data points fell within the 90% prediction intervals, providing further support for the model's predictive accuracy.

Table 2 The Characteristics of Enrolled Patients in Different Subgroups in Exposure-Efficacy Analysis

	VEN + HMA	
	Newly Diagnosed	**R/R**
No. of patients	32	20
Age (year)	9 (2~17)	8 (3~15)
Sex		
Male	13 (40.6%)	15 (75.0%)
Female	19 (59.4%)	5 (25.0%)
Weight (kg)	45 (10~112)	40 (11.5~67.5)
Height (cm)	158.5 (76~190)	151 (93~175)
BMI (kg/m^2)	17.4 (13~36.2)	16.2 (12.2~24)
BSA (m^2)	1.41 (0.44~2.35)	1.3 (0.56~1.75)
C_0 (ng/mL)	1658.15 (131.88~3435.18)	2449.28 (1066.41~7069.28)
C_6 (ng/mL)	3247.46 (743.98~7347.33)	3016.74 (1281.32~10,289.06)
ORR%	32 (100.0%)	18 (90.0%)
MRD (-) %	25 (78.1%)	13 (65.0%)

Table 3 Final PPK Model: Pharmacokinetic Parameter Estimates and Bootstrap Results

Parameter Estimation				Bootstrap	
Parameter	**Estimate**	**RSE%**	**95% CI**	**Median**	**95% CI**
k_a, h^{-1}	0.15 (fixed)			0.15 (fixed)	
V/F, L	124.7	15.0	87.8–161.7	125.4	80.7–183.6
TP on V/F	1.7	24.4	0.9–2.5	1.7	0.6–2.9
CL/F, L/h	4.8	26.5	2.3–7.3	4.9	2.9–10.1
BSA on CL/F	1.4	18.4	0.9–2.0	1.5	0.9–2.6
Triazole on CL/F	−1.1	−34.4	−1.9 to −0.4	−1.1	−2.6 to −0.5
Interindividual variability					
$\omega_{CL/F}$	0.996	17.6	0.2–0.5	1.012	0.5–1.6
$\omega_{V/F}$	0.608	22.6	0.6–1.3	0.612	0.1–0.7
Random residual variability					
σ	0.38	8.5	0.3–0.4	0.37	0.3–0.4

Abbreviations: V/F, apparent volume of distribution; CL/F, Clearance of compartment; TP, total protein; BSA, body surface area.

The external validation dataset consisted of 84 VEN trough concentrations from 39 pediatric patients (refer to Supplementary Table S2). The observed bias, reflected by the MPE of 17.7% and MAE of 28.0%, indicates that the final population model possesses satisfactory predictive capabilities.

Exposure-Efficacy Results

Comparative analyses were performed between MRD-negative and MRD-positive subgroups within both newly diagnosed and R/R cohorts for VEN C_0 and C_6 concentrations (Figure 3). The results demonstrated statistically significant differences in both venetoclax C_0 and C_6 levels between MRD-negative and MRD-positive subgroups. For VEN C_0, in the newly diagnosed group, MRD-negative patients showed significantly higher C_0 levels than MRD-positive patients (1860.6 ± 691.9 ng/mL vs 1145.1 ± 805.7 ng/mL, p = 0.026). Similarly in the R/R group, MRD-negative patients exhibited significantly higher C_0 levels (3486.5 ± 1560.1 ng/mL vs 1838.2 ± 562.0 ng/mL, p = 0.015). For VEN C_6, in the newly diagnosed group, MRD-negative patients demonstrated significantly higher C_6 levels (3380.7 ± 1388.6 ng/mL vs 2075.4 ± 1071.3 ng/mL, p = 0.029). The R/R group showed the same pattern with significantly higher C_6 levels in MRD-negative patients (4540.7 ± 2238.7 ng/mL vs 2200.6 ± 476.0 ng/mL, p = 0.015).

After categorizing C_0 and C_6 by quartiles, the exposure-efficacy relationships based on this quartile analysis are shown in Figures 4 and 5. In the newly diagnosed group, neither the C_0 nor C_6 quartile groups showed a significant association with MRD status (C_0: p=0.176; C_6: p=0.176). In the R/R group, no significant association was observed between C_0 quartiles and MRD status (p=0.115). However, analysis of C_6 quartiles revealed that higher C_6 concentrations were significantly associated with achieving MRD negativity (p=0.011).

First, correlation analyses were conducted between VEN concentrations (C_0, C_6), age, sex, and MRD-negative status in the newly diagnosed and R/R groups, respectively. The results showed that in both the newly diagnosed and R/R groups, VEN C_0 and C_6 levels were significantly positively correlated with achieving MRD-negative status ($p < 0.05$). However, neither age nor sex showed a significant correlation with MRD negativity in either patient group. No statistically significant disparities in age or sex distribution were observed between MRD-positive and MRD-negative cohorts, regardless of whether they were in the newly diagnosed or R/R group. Single-factor logistic regression analysis was first performed for age, sex, C_0, and C_6 with MRD-negativity status; results are presented in Table 4. The analysis revealed a statistically significant positive correlation between VEN concentrations (C_0 and C_6) and MRD-negativity. In the newly diagnosed group, both C_0 (OR=1.002, p=0.046) and C_6 (OR=1.001, p=0.038) showed significant positive correlations with MRD-negativity. Similarly, in the R/R group, both C_0 (OR=1.002, p=0.047) and C_6 (OR=1.002, p=0.044) demonstrated significant positive correlations. Although the ORs were numerically close to 1, this largely

https://doi.org/10.2147/DDDT.S583847

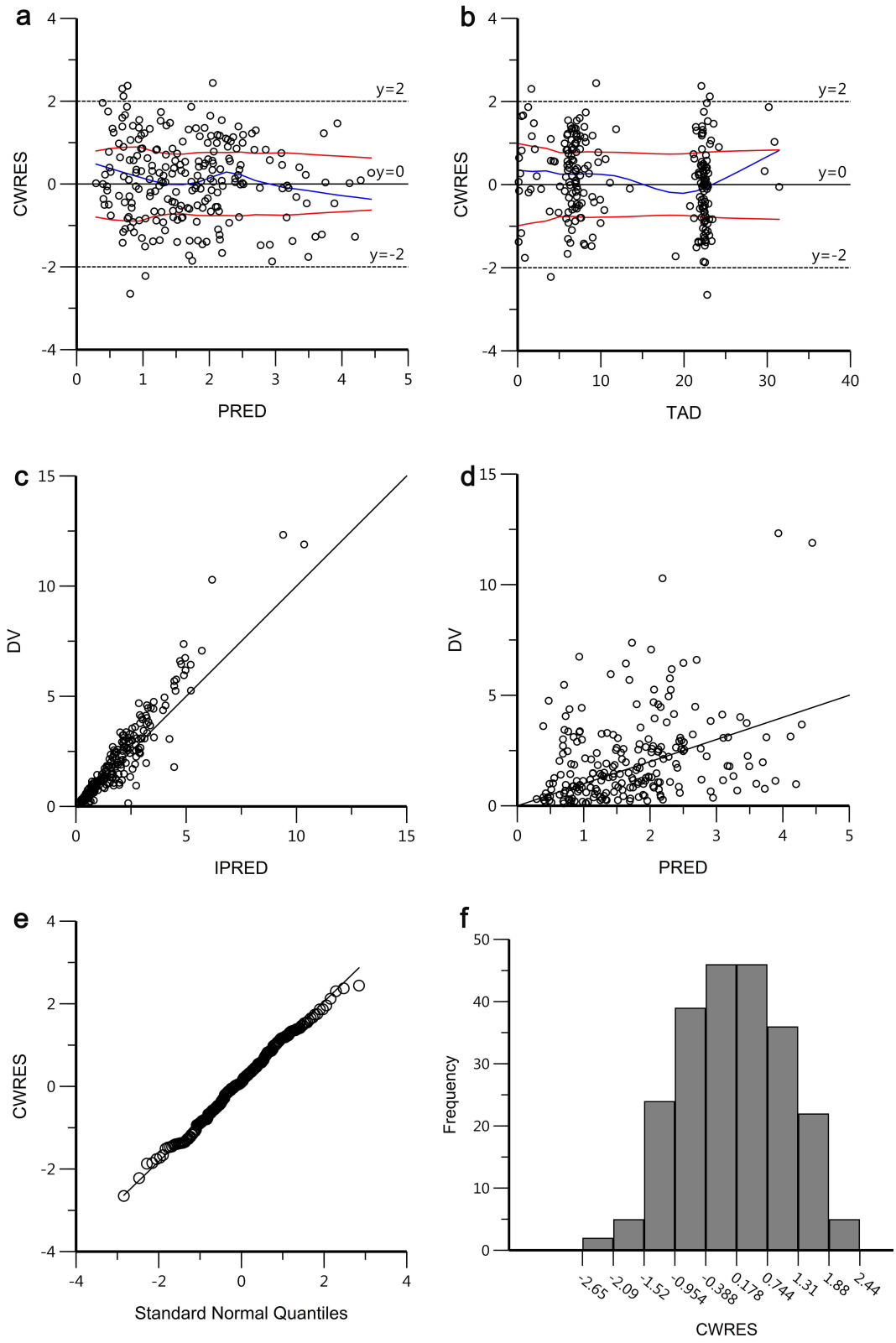

Figure 1 The goodness-of-fit plots for the final (**a**–**f**) pharmacokinetic model. (**a**) CWRES versus PRED; (**b**) CWRES versus TAD; (**c**) DV versus IPRED, the lines indicate the lines of unity y = x; (**d**) DV versus PRED, the lines indicate the lines of unity y = x; (**e**) QQ plots of CWRES; (**f**) histogram of CWRES.
Abbreviations: CWRES, conditional weighted residuals errors; PRED, population predictions; TAD, time after dose; DV, observations; IPRED, individual predictions; QQ, quantile–quantile.

https://doi.org/10.2147/DDDT.S583847

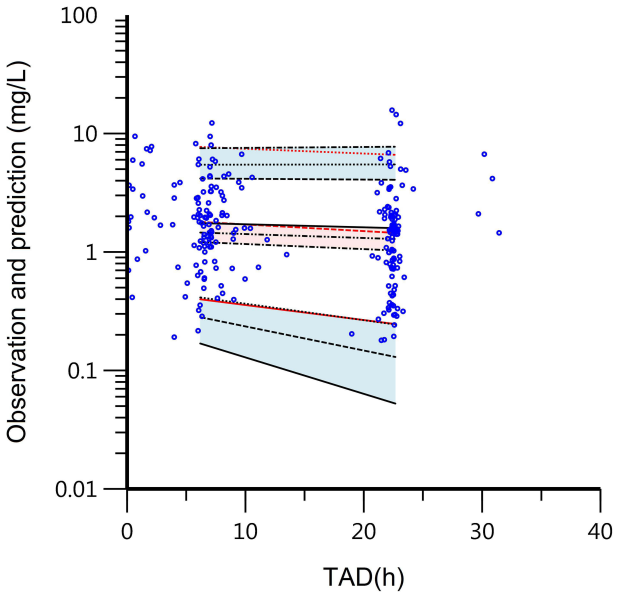

Figure 2 Visual predictive check (VPC) plots from the final model. The circles are the actual observations. The black solid line means the predicted 50% quantile, and the black dashed lines are the predicted 5 and 95% quantiles, indicating the areas between the 5 and 95% quantiles representing the 90% prediction interval. The red solid line is the observed 50% quantile, and the 5 and 95% quantiles are presented with red dashed lines.
Abbreviation: TAD, time after dose.

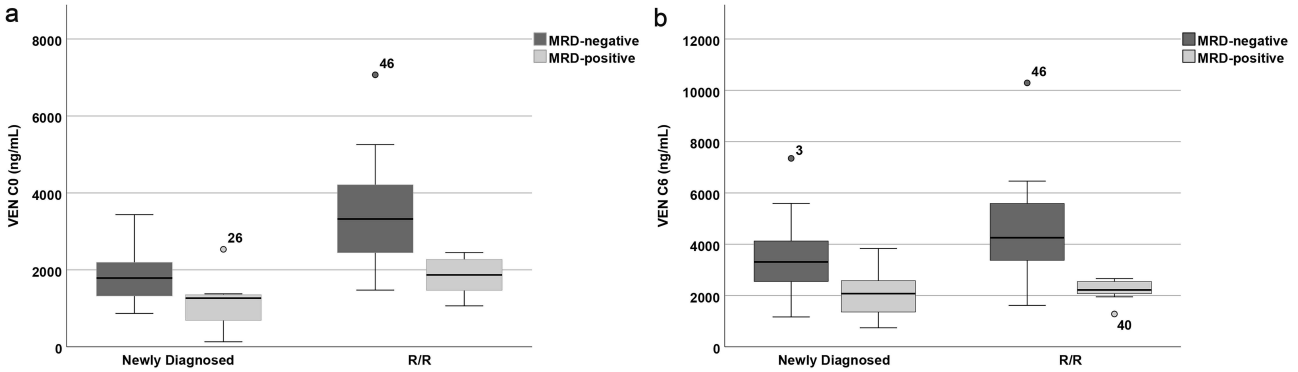

Figure 3 VEN concentrations in newly diagnosed vs R/R patient groups. (**a**) VEN C_0 (ng/mL); (**b**) VEN C_6 (ng/mL).

reflects the use of ng/mL as the unit of measurement. Given the large clinical range of venetoclax concentrations, even small per-unit increases can accumulate to clinically meaningful changes in outcomes.

Discussion

To our knowledge, this is the first study examining the PPK properties of VEN in a cohort of Chinese pediatric patients using real-world data. Unlike our previously published study, which focused on clinical efficacy and safety outcomes of venetoclax-based regimens in pediatric patients with relapsed or refractory acute lymphoblastic leukemia without pharmacokinetic analyses,[21] the current study provides a comprehensive PPK model, explores exposure–response relationships, and supports individualized dosing strategies. So far, six published PPK articles in adult populations[20] and one PPK article in pediatric populations[19] have all used clinical trial data to establish a two-compartment model. Using the population data collected at our center, we conducted simulations based on the pediatric population PPK model parameters reported in the literature. Under limited conditions, since the published literature[19] did not explicitly provide the median weight value, we used the mean and mean ± standard deviation (Mean ± SD) as input parameters for simulation analysis. However, the simulation results showed poor fitting performance, indicating that the model might

https://doi.org/10.2147/DDDT.S583847

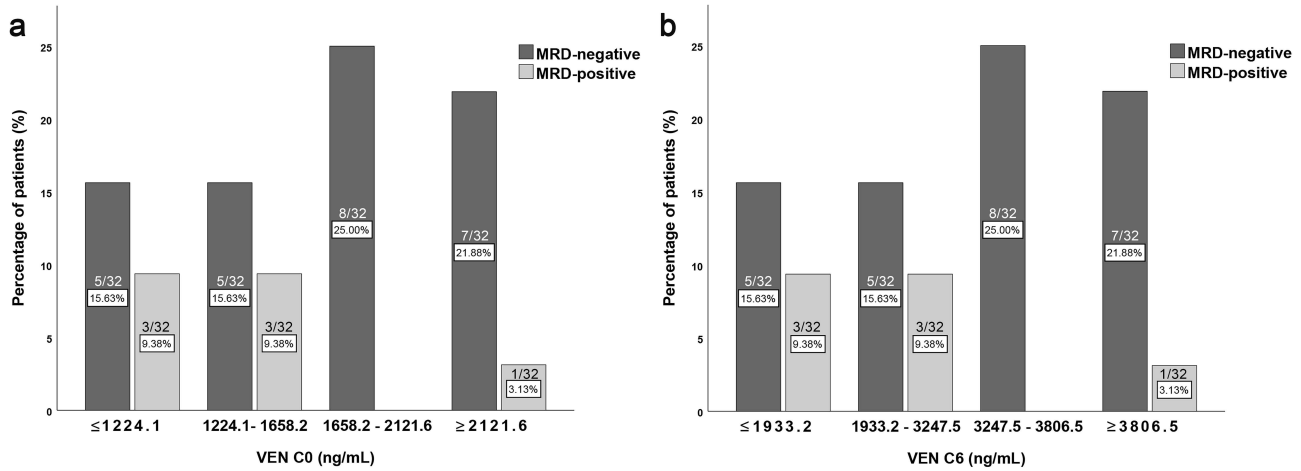

Figure 4 Quartile exposure–response analysis of venetoclax concentrations and MRD status in newly diagnosed patients. (**a**) Association between VEN C_0 quartiles and MRD status. (**b**) Association between VEN C_6 quartiles and MRD status.

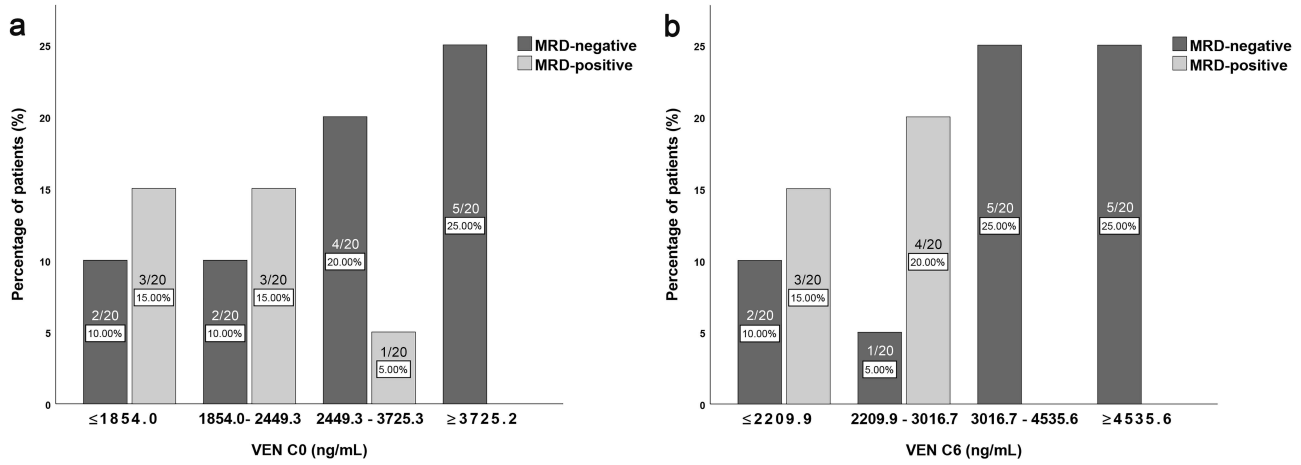

Figure 5 Quartile exposure–response analysis of venetoclax concentrations and MRD status in R/R patients. (**a**) Association between VEN C_0 quartiles and MRD status. (**b**) Association between VEN C_6 quartiles and MRD status.

not be suitable for the population characteristics of our center. Based on this, we further developed a VEN PPK model tailored to the population of our center, aiming to more accurately describe the pharmacokinetic behavior of the VEN in pediatric patients in our region and to provide a scientific basis for the development of individualized dosing regimens.

Based on analysis of the data from 96 patients, we ultimately chose a one-compartment model, which was determined by taking into account the structure of the included data and comparing it with the two-compartment model. Our plasma concentration data of VEN has fewer absorption phases, and we therefore fixed the k_a. We also tried the two-

Table 4 Single-Factor Logistic Regression Results for Venetoclax Exposure Associated with Clinical Response

Endpoint	Group	Exposure Metric	P value	OR (95% CI)*
Minimal residual disease	Newly diagnosed	C_0	0.046(+)	1.002 (1.000–1.003)
		C_6	0.038(+)	1.001 (1.000–1.002)
	R/R	C_0	0.047(+)	1.002 (1.000–1.004)
		C_6	0.044(+)	1.002 (1.000–1.003)

Abbreviations: (+), positive correlation; OR, odds ratio; 95% CI, 95% Confidence Interval.

compartment model, and there was no significant difference in −2LL and AIC between one-compartment and two-compartment models. The two-compartment did not improve fitting effect of the one-compartment model. The V/F and CL/F were estimated at 124.7 L and 4.8 $L \cdot h^{-1}$, respectively. The CL/F estimate in this study is comparatively lower than those reported in previous research. Compared with early investigations, the estimated value of CL/F in this study is relatively low. The potential reasons include the small stature of Chinese patients (the average weight and BSA of Chinese people are relatively smaller), and the genetic polymorphism of metabolic enzymes, etc., which lead to the decrease of CL/F. Following model selection procedures incorporating physiological plausibility assessments, the final PPK model included covariate effects of Triazole and BSA on CL/F, and of TP on V/F.

VEN undergoes primary metabolic clearance through the CYP3A4 enzyme pathway and is also transported as a substrate of P-glycoprotein (P-gp).[27] Patients with hematological malignancies are at a high risk of fungal infection due to chemotherapy and neutropenia.[28,29] For these patients, triazole is often used for the prevention and treatment of fungal infection.[30] In our study, all patients who received triazole antifungal therapy were treated with either posaconazole or voriconazole, which are strong CYP3A inhibitors, they could slow down VEN metabolism, prolong the duration of action, and enhance pharmacological activity or toxic side effects. The co-combination could increase the C_{max} and area under curve (AUC) of VEN and may increase the risk of tumor lysis syndrome (TLS) and other toxic effects, at initiation and during the dose-titration phase.[31] This would need to be considered when potential VEN dose adjustments may be needed. During the ramp-up phase, strong CYP3A4 inhibitors are prohibited, and thereafter the dose of VEN is reduced by at least 75%. If the risk of TLS is low, it may be considered to reduce the dose of VEN during the ramp-up phase (reducing the dose by 75% to 25% of the standard dose).[32] During the ramp-up period, co-administration with moderate CYP3A4 inhibitors necessitates a minimum 50% reduction in the VEN dose to mitigate the risk of increased drug exposure.[33]

Considering the clinical practice where VEN is dosed based on BSA (120 mg/m^2 on day 1 and 240 mg/m^2 on days 2–28 when not co-administered with azole drugs), we included BSA as a covariate rather than height and weight separately. In our study, BSA was calculated by Stevenson formula,[34] which is 0.0061*height(cm) + 0.0128*weight (kg)-0.1529. According to the clearance formula in the final model, the higher the BSA, the greater the clearance rate. Metabolic clearance is governed by regional hepatic blood flow, the extraction efficiency, and the intrinsic metabolic capacity of hepatic enzymes,[35] all of which may vary with developmental age.[24] The extraction efficiency is primarily determined by the unbound fraction of the drug in circulation. In neonates and young children, the liver-to-body weight ratio is elevated compared to older individuals, gradually declining with age. Similarly, hepatic blood perfusion is markedly increased during infancy and early childhood, reflecting age-dependent physiological variation. Research indicates that there is a linear relationship between blood volume and BSA. This means that individuals with a larger BSA typically have a greater blood volume, which will also affect its clearance rate. Individuals with a larger BSA typically have larger metabolic organs, which may function more efficiently, thereby affecting the metabolism and excretion of drugs. VEN is primarily metabolized by CYP3A, and if individuals with a larger BSA have stronger metabolic organ functions, it may accelerate the metabolism of the drug, thereby increasing the clearance rate. It is recommended that patients with higher BSA may require increased VEN dosage. In Badawi et al's study,[19] they incorporated a CYP3A maturation function into the model to account for age-dependent CYP3A maturation and its impact on VEN clearance. Because of Phoenix NLME software reasons, we did not do it this way.

TP was an independent covariate on V/F of VEN in the final model. Low TP levels lead to decreased binding, resulting in higher free drug concentrations in the blood. The equation V=D/C shows that a higher concentration (C) with a given dose (D) implies a smaller volume of distribution (V). VEN is highly bound to human plasma proteins, with a plasma unbound fraction of less than 0.01, which make it difficult to cross the blood-brain barrier (BBB). There have been some case reports[36,37] and pharmacokinetic analysis[38] of VEN penetrating the BBB and improving the central nervous system involvement in leukemia. Further research is necessary to determine VEN' s potential effectiveness in improving clinical outcomes. After increasing the number of cerebrospinal fluid (CSF) samples sufficiently, it may be possible to attempt the development of a PPK model of CSF to blood clearance.

VEN exposure levels demonstrated significant correlations with MRD status. In both newly diagnosed and R/R groups, MRD-negative patients exhibited significantly higher VEN C_0 and C_6 concentrations compared to MRD-positive patients ($p<0.05$). These findings suggest that higher VEN exposure may promote deeper disease remission through

enhanced target engagement or prolonged pharmacological activity. Existing studies support the association between VEN trough concentrations and MRD status. Based on the phase Ib clinical trial (NCT02203773) of VEN-HMAs and pivotal pharmacokinetic studies, Wang et al[18] defined the reference ranges for VEN trough and peak concentrations as 0.5–4 μg/mL and 2.0–5.5 μg/mL, respectively.[10,27,39,40] Their results demonstrated significantly higher MRD-negative rates in patients with C_0 within the reference range compared to those outside the range (90.91% vs 33.33%, p=0.028), suggesting that maintaining effective C_0 is crucial for achieving better responses. These findings align with our current study, where MRD-negative patients in both newly diagnosed (1860.6 vs 1145.1 ng/mL, p=0.026) and R/R groups (3486.5 vs 1838.2 ng/mL, p=0.015) showed significantly higher C_0. The therapeutic trough concentrations may continuously inhibit BCL-2 protein, thereby enhancing leukemic cell apoptosis and improving MRD status. Furthermore, our logistic regression analysis confirmed statistically significant positive correlations between both VEN concentrations (C_0 and C_6) and MRD negativity.

This study did not proceed with a multivariate logistic regression analysis incorporating age, sex, and venetoclax concentration, primarily for the following reasons: First, previous key cohort studies in children and adults did not systematically analyze age or sex as independent influencing factors for MRD negativity.[18] Second, this study observed no significant differences in age or sex distribution between MRD-positive and MRD-negative patients in either the newly diagnosed or R/R groups. Preliminary correlation analyses also indicated that neither age nor sex showed a significant association with MRD-negative status in either group. Given that these demographic variables lacked prior supporting evidence and showed no indications of association with MRD-negative status in either the inter-group comparisons or correlation analyses within this cohort, such analysis was not pursued.

Our study has several limitations, including the following: (1) sparse sampling points in patients may affect parameter estimation, and considering the feasibility of the sampling scheme in clinical practice, there are fewer sample points during the absorption phase. Therefore, we fixed the k_a in the model; (2) the sample size may be insufficient to adequately assess the influence of covariates, such as the impact of renal function, liver function, and inflammatory markers (procalcitonin, C-reactive protein), which requires more samples for validation; (3) uncontrollable confounding factors, such as comedications, are inherent in patient populations and cannot be avoided in real-world studies; (4) the proposed model needs to be tested in practice; (5) most enrolled patients have normal liver and kidney function levels, and because most patients are co-administered with triazole antifungal drugs, inflammatory markers are mostly normal, making it difficult to adequately assess the impact of the aforementioned factors; (6) The interpretation of exposure-efficacy relationships may be confounded by uncontrolled factors such as BCL-2 expression levels, drug combination, or genetic variations. In addition, due to limitations in follow-up, this study did not systematically collect safety outcomes including hematologic toxicities and infection events, thereby precluding a thorough evaluation of the relationship between drug concentrations and toxicity.

Conclusion

In summary, we established a PPK model for VEN in Chinese pediatric patients, identifying three pivotal covariates: BSA and triazole coadministration affecting CL/F, and TP influencing V/F. Exposure-efficacy analysis demonstrates significant differences in the relationships of VEN C_0 and C_6 across different treatment phases, revealing a distinct correlation between VEN concentration levels and MRD status. These findings highlight the potential of PPK-guided dosing strategies and therapeutic drug monitoring to support individualized therapy, optimize clinical efficacy, and improve long-term outcomes in pediatric leukemia management. Future multicenter studies are warranted to externally validate and enhance the generalizability of the model.

Data Sharing Statement

The datasets generated and/or analyzed during the current study are not publicly available due to patient privacy and institutional restrictions but may be made available from the corresponding author upon reasonable request.

Author Contributions

All authors made a significant contribution to the work reported, whether that is in the conception, study design, execution, acquisition of data, analysis and interpretation, or in all these areas; took part in drafting, revising or critically reviewing the article; gave final approval of the version to be published; have agreed on the journal to which the article has been submitted; and agree to be accountable for all aspects of the work.

Funding

This work was supported by the Beijing Municipal Natural Science Foundation (grant number 7242210).

Disclosure

The authors declare that they have no conflicts of interest in this work.

References

1. Souers AJ, Leverson JD, Boghaert ER, et al. ABT-199, a potent and selective BCL-2 inhibitor, achieves antitumor activity while sparing platelets. *Nat Med*. 2013;19(2):202–208. doi:10.1038/nm.3048
2. Pullarkat VA, Lacayo NJ, Jabbour E, et al. Venetoclax and navitoclax in combination with chemotherapy in patients with relapsed or refractory acute lymphoblastic leukemia and lymphoblastic lymphoma. *Cancer Discov*. 2021;11(6):1440–1453. doi:10.1158/2159-8290.CD-20-1465
3. Karol SE, Alexander TB, Budhraja A, et al. Venetoclax in combination with cytarabine with or without idarubicin in children with relapsed or refractory acute myeloid leukaemia: a phase 1, dose-escalation study. *Lancet Oncol*. 2020;21(4):551–560. doi:10.1016/s1470-2045(20)30060-7
4. Place AE, Goldsmith K, Bourquin JP, et al. Accelerating drug development in pediatric cancer: a novel Phase I study design of venetoclax in relapsed/refractory malignancies. *Future Oncol*. 2018;14(21):2115–2129. doi:10.2217/fon-2018-0121
5. Wilson A, Moussa A, Trinquand A, et al. Real-world use of venetoclax in the treatment of paediatric and teenage/young adult haematological malignancies. *Br J Haematol*. 2024;205(6):2355–2362. doi:10.1111/bjh.19791
6. Gibson A, Dickson S, McCall D, et al. Venetoclax for pediatric patients with newly diagnosed acute myeloid leukemia. *Pediatr Blood Cancer*. 2024;71(11):e31286. doi:10.1002/pbc.31286
7. LeBlanc FR, Breese EH, Burns KC, et al. Clinical outcomes of hypomethylating agents and venetoclax in newly diagnosed unfit and relapsed/refractory paediatric, adolescent and young adult acute myeloid leukaemia patients. *Br J Haematol*. 2024;205(3):1055–1066. doi:10.1111/bjh.19679
8. The Subspecialty Group of Pediatric Hematology and Oncology, Pediatric Medical Doctor Society of the Chinese Medical Doctor Association; the Subspecialty Group of Hematology, Society of Pediatrics, Chinese Medical Association. Expert consensus on the diagnosis and treatment of pediatric acute myeloid leukemia (2024). *Chin J Pediatr*. 2024;62(10):909–919. doi:10.3760/cma.j.cn112140-20240722-00500
9. NCCN clinical practice guidelines in oncology pediatric acute lymphoblastic leukemia. Version 1.2024. 2024.
10. DiNardo CD, Pratz KW, Letai A, et al. Safety and preliminary efficacy of venetoclax with decitabine or azacitidine in elderly patients with previously untreated acute myeloid leukaemia: a non-randomised, open-label, phase 1b study. *Lancet Oncol*. 2018;19(2):216–228. doi:10.1016/S1470-2045(18)30010-X
11. Freise KJ, Shebley M, Salem AH. Quantitative prediction of the effect of CYP3A inhibitors and inducers on venetoclax pharmacokinetics using a physiologically based pharmacokinetic model. *J Clin Pharmacol*. 2017;57(6):796–804. doi:10.1002/jcph.858
12. Kaufman JL, Gasparetto C, Schjesvold FH, et al. Targeting BCL-2 with venetoclax and dexamethasone in patients with relapsed/refractory t(11;14) multiple myeloma. *Am J Hematol*. 2021;96(4):418–427. doi:10.1002/ajh.26083
13. Freise KJ, Jones AK, Eckert D, et al. Impact of venetoclax exposure on clinical efficacy and safety in patients with relapsed or refractory chronic lymphocytic leukemia. *Clin Pharmacokinet*. 2017;56(5):515–523. doi:10.1007/s40262-016-0453-9
14. Agarwal S, Gopalakrishnan S, Mensing S, et al. Optimizing venetoclax dose in combination with low intensive therapies in elderly patients with newly diagnosed acute myeloid leukemia: an exposure-response analysis. *Hematol Oncol*. 2019;37(4):464–473. doi:10.1002/hon.2646
15. Badawi M, Coppola S, Eckert D, et al. Venetoclax in biomarker-selected multiple myeloma patients: impact of exposure on clinical efficacy and safety. *Hematol Oncol*. 2024;42(1):e3222. doi:10.1002/hon.3222
16. Yan Y, Guo Y, Wang Z, et al. Clinical pharmacology and side effects of venetoclax in hematologic malignancies. *Curr Drug Metab*. 2024. doi:10.2174/0113892002338926241114080504
17. AbbVie Inc. VENCLEXTA (venetoclax) [package insert]. U.S. Food and Drug Administration website. Available from: https://www.accessdata.fda.gov/drugsatfda_docs/label/2018/208573s009lbl.pdf. (2018). Accessed March 6, 2026.
18. Wang L, Gao L, Liang Z, Cen X, Ren H, Dong Y. Efficacy and safety of coadministration of venetoclax and anti-fungal agents under therapeutic drug monitor in unfit acute myeloid leukemia and high-risk myelodysplastic syndrome with neutropenia: a single-center retrospective study. *Leuk Lymphoma*. 2024;65(3):353–362. doi:10.1080/10428194.2023.2290465
19. Badawi M, Gopalakrishnan S, Engelhardt B, et al. Dosing of venetoclax in pediatric patients with relapsed acute myeloid leukemia: analysis of developmental pharmacokinetics and exposure-response relationships. *Clin Ther*. 2024;46(10):759–767. doi:10.1016/j.clinthera.2024.09.008
20. Zhao Y, Guo N, Zhu Y, et al. Population pharmacokinetic models of venetoclax in hematologic malignancies: a systematic review. *Drug Des Devel Ther*. 2024;18:1771–1784. doi:10.2147/DDDT.S458927
21. Zhang L, Zhang Z, Lu A, et al. Venetoclax-Based regimen in refractory or relapsed pediatric acute lymphoblastic leukemia. *Acta Haematol*. 2025. doi:10.1159/000547080
22. Levey AS, Stevens LA, Schmid CH, et al. A new equation to estimate glomerular filtration rate. *Ann Intern Med*. 2009;150(9):604–612. doi:10.7326/0003-4819-150-9-200905050-00006

23. Jones AK, Freise KJ, Agarwal SK, Humerickhouse RA, Wong SL, Salem AH. Clinical predictors of venetoclax pharmacokinetics in chronic lymphocytic leukemia and non-hodgkin's lymphoma patients: a pooled population pharmacokinetic analysis. *AAPS J*. 2016;18(5):1192–1202. doi:10.1208/s12248-016-9927-9
24. van den Anker J, Reed MD, Allegaert K, Kearns GL. Developmental changes in pharmacokinetics and pharmacodynamics. *J Clin Pharmacol*. 2018;58 Suppl 10:S10–S25. doi:10.1002/jcph.1284
25. Bloomfield C, Staatz CE, Unwin S, Hennig S. Assessing predictive performance of published population pharmacokinetic models of intravenous tobramycin in pediatric patients. *Antimicrob Agents Chemother*. 2016;60(6):3407–3414. doi:10.1128/AAC.02654-15
26. Hara M, Masui K, Eleveld DJ, Struys M, Uchida O. Predictive performance of eleven pharmacokinetic models for propofol infusion in children for long-duration anaesthesia. *Br J Anaesth*. 2017;118(3):415–423. doi:10.1093/bja/aex007
27. Agarwal SK, DiNardo CD, Potluri J, et al. Management of venetoclax-posaconazole interaction in acute myeloid leukemia patients: evaluation of dose adjustments. *Clin Ther*. 2017;39(2):359–367. doi:10.1016/j.clinthera.2017.01.003
28. Hahn-Ast C, Glasmacher A, Mückter S, et al. Overall survival and fungal infection-related mortality in patients with invasive fungal infection and neutropenia after myelosuppressive chemotherapy in a tertiary care centre from 1995 to 2006. *J Antimicrob Chemother*. 2010;65(4):761–768. doi:10.1093/jac/dkp507
29. Pagano L, Caira M, Candoni A, et al. The epidemiology of fungal infections in patients with hematologic malignancies: the SEIFEM-2004 study. *Haematologica*. 2006;91(8):1068–1075.
30. Guarana M, Nucci M. Should patients with acute myeloid leukemia treated with venetoclax-based regimens receive antifungal prophylaxis? *Leuk Res*. 2023;131:107341. doi:10.1016/j.leukres.2023.107341
31. Dong J, Liu SB, Rasheduzzaman JM, Huang CR, Miao LY. Development of physiology based pharmacokinetic model to predict the drug interactions of voriconazole and venetoclax. *Pharm Res*. 2022;39(8):1921–1933. doi:10.1007/s11095-022-03289-9
32. Azanza JR, Mensa J, Barberan J, et al. Recommendations on the use of azole antifungals in hematology-oncology patients. *Rev Esp Quimioter*. 2023;36(3):236–258. doi:10.37201/req/013.2023
33. Bruggemann RJ, Verheggen R, Boerrigter E, et al. Management of drug-drug interactions of targeted therapies for haematological malignancies and triazole antifungal drugs. *Lancet Haematol*. 2022;9(1):e58–e72. doi:10.1016/S2352-3026(21)00232-5
34. Stevenson PH. Calculation of the body-surface area of Chinese. *Chin J Physiol*. 1928: 13–24.
35. Hines RN. Developmental expression of drug metabolizing enzymes: impact on disposition in neonates and young children. *Int J Pharm*. 2013;452 (1–2):3–7. doi:10.1016/j.ijpharm.2012.05.079
36. Condorelli A, Matteo C, Leotta S, et al. Venetoclax penetrates in cerebrospinal fluid of an acute myeloid leukemia patient with leptomeningeal involvement. *Cancer Chemother Pharmacol*. 2022;89(2):267–270. doi:10.1007/s00280-021-04356-5
37. Zhang X, Chen J, Wang W, et al. Treatment of central nervous system relapse in acute promyelocytic leukemia by venetoclax: a case report. *Front Oncol*. 2021;11:693670. doi:10.3389/fonc.2021.693670
38. Badawi M, Menon R, Place AE, et al. Venetoclax penetrates the blood brain barrier: a pharmacokinetic analysis in pediatric leukemia patients. *J Cancer*. 2023;14(7):1151–1156. doi:10.7150/jca.81795
39. Brackman D, Eckert D, Menon R, et al. Venetoclax exposure-efficacy and exposure-safety relationships in patients with treatment-naive acute myeloid leukemia who are ineligible for intensive chemotherapy. *Hematol Oncol*. 2022;40(2):269–279. doi:10.1002/hon.2964
40. Yang X, Mei C, He X, et al. Quantification of venetoclax for therapeutic drug monitoring in chinese acute myeloid leukemia patients by a validated UPLC-MS/MS method. *Molecules*. 2022;27(5). doi:10.3390/molecules27051607